Laser Surface-contouring and Spline Data-smoothing for Residual Stress Measurement

by M.B. Prime, R.J. Sebring, J.M. Edwards, D.J. Hughes and P.J. Webster

ABSTRACT—We describe non-contact scanning with a con-focal laser probe to measure surface contours for application to residual stress measurement. (In the recently introduced contour method, a part is cut in two with a flat cut, and the part deforms by relaxation of the residual stresses. A cross-sectional map of residual stresses is then determined from measurement of the contours of the cut surfaces.) The contour method using laser scanning is validated by comparing measurements on a ferritic steel (BS 4360 grade 50D) weldment with neutron diffraction measurements on an identical specimen. Compared to lower resolution touch probe techniques, laser surface-contouring allows more accurate measurement of residual stresses and/or measurement of smaller parts or parts with lower stress levels. Furthermore, to take full advantage of improved spatial resolution of the laser measurements, a method to smooth the surface contour data using bivariate splines is developed. In contrast to previous methods, the spline method objectively selects the amount of smoothing and estimates the uncertainties in the calculated residual stress map.

KEY WORDS—Residual stresses, contour method, coordinate measuring machine, wire EDM, TIG weld, model error

Introduction

Recently a new method for measuring residual stress, the contour method, has been introduced.[1,2] In the contour method, a part is carefully cut in two along a flat plane causing the residual stresses normal to the cut plane to relax. The contour of each of the opposing surfaces created by the cut is then measured. The deviation of the surface contours from planarity is assumed to be caused by elastic relaxation of the residual stresses and is therefore used to calculate the original residual stresses. One of the unique strengths of the contour method is that it provides a full cross-sectional (two-dimensional) map of the residual stress component normal to the cross-section. Other relaxation methods, at least those that are commonly used, determine at most a one-dimensional

depth profile,[3] although some can measure multiple stress components.[4]

In all applications of the contour method to date, the surface contours were measured using a touch probe on a commercial Coordinate Measuring Machine (CMM).[5–7] A CMM is a device commonly used to inspect machined parts for dimensional accuracy, and the touch probe determines surface location by contacting the surface. The accuracy of residual stress maps produced using the contour method with a touch probe CMM measurement of the surface contours has been demonstrated by measuring a specimen with known residual stresses.[1]

Measuring the surface contours with a touch probe limits the resolution and accuracy of contour method residual stress measurements and also has other disadvantages. The precision and accuracy of the best current touch probes are generally 1–3 μm. The peak-to-valley amplitude of the contour that we would expect to measure for some arbitrary part decreases as the stress magnitude decreases. For a given stress magnitude, the contour amplitude also decreases as the part size decreases because the surface contour is a displacement not a strain. Whereas strain does not scale with part size for a given stress, the contour is the relaxed strain integrated over dimensions of the part and, therefore, scales. Therefore, a more precise and accurate method for measuring a surface contour would potentially allow the measurement of smaller parts or parts with lower stress levels. A second disadvantage of a touch probe is that sampling rates in the most accurate mode are about one measurement point per second, meaning that sampling tens of thousands of points to define a surface can take hours. A third disadvantage is that the probe contact pressure in a vertical orientation will locally deform parts during the measurement and leave permanent marks. In spite of the low contact forces, this deformation occurs because of the small contact area of the probe.

The significant application of laser scanning to residual stress measurement is new. Contouring by scanning with a laser probe is a proven technology that can provide a more accurate surface contour than can a touch probe.[8] Laser contouring has only been applied to residual stress measurement by measuring average gross curvature in thin films to make an estimate of stress profiles.[9] Many interferometric techniques measure displacements and therefore are not applicable to the contour method because the cut surface is not accessible for the undeformed, or "before", portion of a displacement measurement. Most previous applications of lasers to residual stress measurement fall into this category of measuring displacements not contours.[10–12] Full-field measurements of

M.B. Prime (prime@lanl.gov; SEM Member) is a Technical Staff Member, Engineering Sciences and Applications Division, Los Alamos National Laboratory, Los Alamos, NM 87545, USA. R.J. Sebring is a Technical Staff Member, and J.M. Edwards is a Technician, Materials Science and Technology Division, Los Alamos National Laboratory, Los Alamos, NM 87545, USA. D.J. Hughes is a Researcher, FaME38 at ILL-ESRF, 6 rue Jules Horowitz, BP 156, 38042 Grenoble Cedex, France. P.J. Webster is a Professor, Institute for Materials Research, School of Aeronautical, Civil and Mechanical Engineering, University of Salford, Manchester, M5 4WT, UK.

surface contours, compared to scanning, are possible using, for example, shadow moiré.[13,14] However, for the application in this work, the improved accuracy and versatility of laser scanning are more important than the shorter measurement time possible with a full-field technique.

For the contour method, the conventional data analysis approach is unable to take full advantage of the improved spatial resolution of the laser measurements. Before calculating stress, the surface contour data must be smoothed, which was previously done by fitting to a bivariate Fourier series. However, it is difficult to use a single function to fit the more complex surfaces that laser scanning can measure. Furthermore, the amount of smoothing, which was previously selected based on judgment, affects the results. Bivariate spline smoothing is a widely used and effective technique for fitting complex surfaces. However, because the stress calculation procedure magnifies noise in the data, conventional methods for selecting the amount of smoothing based solely on the data fit do not work well. Instead, a selection based on minimizing uncertainty in the final results, the stresses, is warranted.

Validation Specimen

An experiment on a welded plate provided a twofold validation of the use of laser surface contouring for residual stress mapping with the contour method. Comparing the laser contour residual stress map with the same map obtained using neutron diffraction on a nominally identical specimen validated both the laser contouring and the contour method as a whole. Comparing laser results with results obtained on the same specimen when the contour was measured using a touch probe CMM further validated the use of laser contouring for the contour method and also validated the use of touch probes on parts where decreased measurement resolution is acceptable.

Specimen

A welded steel plate was prepared by TWI Ltd, UK for the VAMAS TWA20 program to develop standard procedures for neutron diffraction measurements of residual stress.[15] The material was ferritic steel BS 4360 grade 50D, commonly used in offshore structures and specified to have a minimum yield strength of 355 MPa. The plate prior to welding was $1000 \times 150 \times 12.5$ mm^3. It had been flame cut from a larger sheet, and the rough edges had then been ground to produce reasonably smooth and square edges. An 8 mm wide U-groove was machined to a depth of 8.5 mm in the middle of the plate along its 1000 mm length. A 12-pass TIG weld was made in the groove using a Bostrand MS65 wire, a mild steel metal active gas (MAG) wire used for welding mild and low alloy steels. The manufacturer reports typical as-welded yield strength of the weld wire as 525 MPa. The plate was clamped for the first ten passes but released for the last two. The resulting weldment was bent upwards towards the weld side around the line of the weld at an angle of approximately 7°. Because of flame-cutting variations and restraint during welding, residual stresses near the transverse extremities were not expected to necessarily be close to zero, nor was the residual stress pattern expected to be totally symmetrical. Several 200 mm long, essentially identical samples were cut from the central region of the 1000 mm long plate for a VAMAS round robin. For the study reported in this paper, one of these samples was measured with the contour method and another with neutron diffraction.

Neutron Measurements

The neutron technique determines the elastic lattice strain from the small shift in the angular position of a Bragg diffraction peak that results when polycrystalline materials are strained.[16] Stresses are then calculated using Hooke's law by combining the strains measured in three directions at each point. In this investigation, strain measurements were made in the three orthogonal near-symmetry directions: along the weld, perpendicular in plane, and normal to the plate surface. The Fe (211) reflection was measured using a wavelength of 1.836 Å and gage volumes of $2 \times 2 \times 2$ mm^3 for longitudinal orientation and $2 \times 2 \times 20$ mm^3 for transverse orientation. Measurements were made over the full cross-section using a rectangular scanning matrix of more than 1200 locations. The measurements were made using the L-3 diffractometer at Chalk River Laboratories, Ontario, Canada.

Contour Method Experiment

Part Cutting

The first step in measuring residual stresses with the contour method is to cut the part in two. Currently, the ideal method for making the cut has proven to be wire electric discharge machining (WEDM), a widely used manufacturing process.[17] WEDM is ideal because it makes a very straight cut, does not remove additional material from previously cut surfaces, does not induce plastic deformation, and results in negligible induced stresses if cutting is performed under the proper conditions.[18] A disadvantage is that WEDM can only be used on electrically conductive material.

The weld plate was cut with a Mitsubishi SX-10 WEDM machine using a 100 μm diameter brass wire. The part was submerged in temperature-controlled deionized water throughout the cutting process. "Skim cut" settings, which are normally used for better precision and a finer surface finish, were used because they also minimize any recast layer and cutting-induced stresses.[18] The slit was about 120 μm wide including the overcut.

For the contour method, it is preferred to minimize the amount the cut deviates from the original cut plane. Therefore, the part must be constrained from moving as stresses are relaxed during the cutting. For the weld specimen, such constraint was achieved by clamping the part on both sides of the cut (see Fig. 1) whereas usually for WEDM only one side of the workpiece is clamped. To prevent any thermal stresses, the weld specimen, backing plate, and all the clamps were allowed to come to thermal equilibrium in the water tank before clamping.

Surface Contouring

After unclamping the weldment, laser surface contouring was performed using a custom-built non-contact measuring machine, although similar machines are commercially available. The machine has been described in detail elsewhere,[19] so only its salient features are described here. The motion hardware used for this task consisted of two orthogonal linear axes, designated x-axis and y-axis in Fig. 2. The motions were precision air-bearing slides with non-contact linear
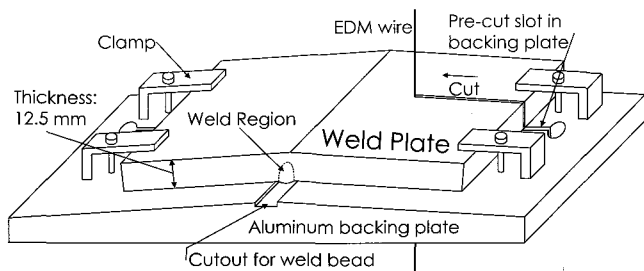
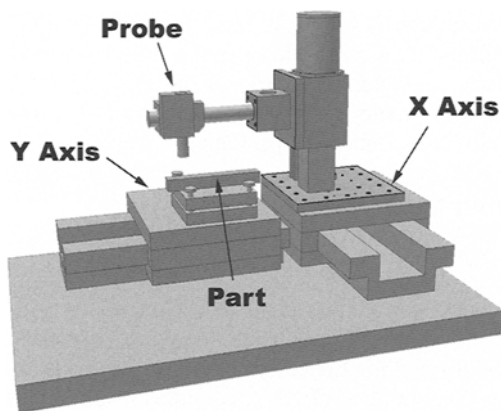Fig. 1—Weld specimen and clamping arrangement for cutting by WEDM

Fig. 2—Setup of laser contouring system, shown with generic part rather than the weld specimen described in this paper

motors. The motions have a linear resolution of 0.1 μm, controlled by a Galil 8-channel controller with a data capture rate of 200,000 samples s^{-1} per eight channels. The system was operated from a PC through a graphical user interface running LabView® software. The welded ferritic steel plate was fixtured on the y-axis stage such that the WEDM cut surface, the surface to be contoured, was facing up. The confocal laser ranging probe (Model LT-8105, Keyence Corp.) was fixtured on the x-axis stage with the laser normal to the cut surface. The laser beam was nominally 7 μm in diameter and the nominal accuracy of the probe was ±0.2 μm. A motion control script was written to generate a raster motion with 0.05 × 0.25 mm point spacing, giving about 200,000 points on the surface. Once initiated, the system ran automatically until complete. The matching surface on the other half of the weldment was scanned in an identical fashion the same day. Raw data, in volts for the probe distance and encoder steps for the $x-y$ motion, were converted to coordinate data in millimeters and automatically stored in a text file as the data were acquired.

For comparison purposes, the surface contour measurements were also taken using a Brown & Sharpe XCEL 765 touch probe CMM. A 4 mm diameter spherical ruby tip was used on the probe. The cut surfaces were measured on a 0.4 mm spaced grid, giving about 12,000 points on each cut surface.

The contours measured on the two halves of the plate were approximately the same shape but not the same amplitude.

On one side, the maximum peak-to-valley distance was about 95 μm with the low spot in the weld region, and on the other side it was about 60 μm. (The measured contours are not plotted in this paper because the large number of data points made it difficult; see Fig. 8 later in the paper for partial data.) The difference between the two surfaces likely occurred because the cut was not centered between the clamps; the clamps on one side of the cut in Fig. 1 were twice as far from the cut as the clamps on the other side. Such asymmetries will cause the material on the plane of the cut to move slightly as stresses are released, leaving a low region on one surface and a corresponding high region on the other. Fortunately, this deviation is antisymmetric with respect to the cut plane and, hence, will not cause errors in the results so long as the two contours are averaged before calculating stress.[1]

Data Analysis

The basic stress calculation procedure is the same as previous applications of the contour method. However, in order to make full use of the more highly resolved surface contour data provided by the laser scanner, it was necessary to improve the way that the data were smoothed. The old method of smoothing the data by fitting to a Fourier series was not able to capture all of the features that could now be resolved in the surface contour. Furthermore, in the past there had been no way to objectively select the amount of smoothing (i.e., the order of the Fourier series) or to estimate the uncertainty in the stress map.

Stress Calculation

The stresses that were originally present on the plane of the cut were calculated numerically by elastically deforming the cut surface into the opposite shape of the contour that was measured on the same surface.[1] This was accomplished using a three-dimensional elastic finite element (FE) model. A model was constructed of one half of the plate, the condition after it had been cut in two. Because the deformations from stress relaxation amounted to less than 1% of the part dimensions, the undeformed state (including a flat cut surface) was modeled. Using the commercial code ABAQUS, the model used reduced integration, quadratic shape-function (i.e., 20 node) brick elements. The elements were cubes approximately 1 mm on a side, resulting in 97,500 elements, 420,727 nodes and 1,262,181 degrees of freedom. The material behavior was isotropic linearly elastic with a Young's modulus of 209 GPa and a Poisson ratio of 0.3. For the stress calculation, the opposite of the measured surface contour was applied as z-direction displacement boundary conditions on the surface corresponding to the cut. Because the measured contours give no information about transverse deformations, the transverse (x and y) displacements were left unconstrained in the FE model, which means that the FE analysis enforces the condition that τ_{xz} and τ_{yz} be zero on the surface. As was demonstrated previously, the correct result for σ_z was returned, even if τ_{xz} and τ_{yz} were non-zero, so long as the two contours were averaged.[1] Finally, to prevent rigid body motions in the $x-y$ plane and the accompanying numerical singularities, three additional displacement constraints were applied and later confirmed to induce no reaction forces. Figure 3 shows the FE model after it was deformed into the opposite shape of the measured contour.
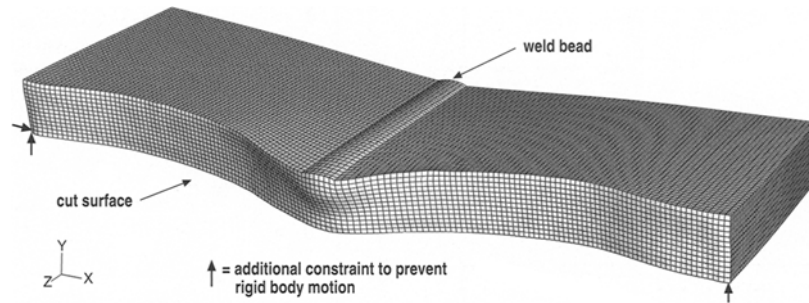
Fig. 3—FE model used to calculate residual stresses from data, with deformations magnified by 200. The cut surface has been deformed into the opposite shape of the measured surface contour

Seven steps were used to process the discrete surface contour data, i.e., the point clouds, into a form suitable for calculating the stresses with the FE model.

1. Because the local coordinate systems used to measure the two cut surfaces were different, the point cloud from one surface was reoriented, in this case mirrored in the x-direction, to get the two point clouds into the same coordinate system relative to the original part. Then the point clouds were aligned to each other by translating and rotating them in the x–y plane. Because of these operations, the grid point coordinates on one surface were not the same as on the other surface.

2. The planar component of each point cloud was then removed by fitting to a best-fitting plane and then subtracting the plane from the data. The planar component would not result in any residual stresses in the final calculation,[1] but it was removed because it can affect the subsequent data processing.

3. The data sets from the two surfaces were then interpolated, using linear Delaunay triangulation, onto a common grid with approximately the same density as the original data. Uniformly gridded data are necessary for the process used later to smooth the raw data.

4. Regions of missing data around the perimeter of the surface were filled in by extrapolating constant values from the nearest interior point with a defined surface height. Such extrapolation is necessary because the surface contour data invariably fail to extend completely to the perimeter, and the whole surface must be defined because displacements must be applied to all cut surface nodes in the FE model. Stresses calculated in the extrapolated region are not reported. The extrapolation does not significantly affect stresses elsewhere so long as the planar component was removed from the data before extrapolation.[20]

5. The two data sets, now on a common grid, were averaged point by point to provide a single data set. Several potential error sources were minimized by averaging the contours measured on both of the two pieces created by the cut.[1]

6. The data were then smoothed by fitting the data to a surface, which is discussed in detail below.

7. Finally, the z-coordinates of the smoothed surface were evaluated at the x–y locations of the nodes in the finite element model, the signs were reversed, and the results were written into the FE input deck as displacement boundary conditions.

Data Smoothing and Uncertainty Estimation

The data were fit to a surface using bivariate smoothing splines. Smoothing was required because noise in the raw surface data would be amplified into greater noise in the stress map, making it difficult to interpret results. In previous applications of the contour method, fitting to a high-order, continuous, bivariate Fourier series smoothed the data. However, the surface data that are reported here proved difficult to fit adequately with a single Fourier expansion. Hence, it was decided that splines, or piecewise defined and smoothly joined polynomials, would be more appropriate. For this application, bivariate, or tensor product, quadratic smoothing splines were used.[21†] The parameter that determined the amount of smoothing versus the amount of detail in the fit was the spacing between the knots in the splines. The knots were the points where the piecewise polynomials were joined.

The amount of smoothing was objectively chosen by minimizing an estimate of the uncertainty in the calculated stresses. It was expected that there would be an optimum amount of smoothing; an overly smooth fit (too coarse knot spacing) would fail to capture the features in the surface, and an overly detailed fit (too fine knot spacing) would unnecessarily capture noise in the data. Often in similar data reductions, the amount of smoothing is chosen using only subjective judgment.[22] Recently, some success has been reported in selecting how precisely to fit the data, i.e., the amount of smoothing, by minimizing errors in the final results (the stresses), although for a significantly different data reduction process.[23] Selecting the amount of smoothing based on the data fit alone would be simpler because it does not require multiple FE calculations. However, minimizing uncertainty in the stresses could only be achieved by calculating the stresses for different amounts of smoothing.

---

†As in the MATLAB® demonstration tspdem in the spline toolbox, we use the command spap2({knotsy,knotsx},[k k],{y, x},Z). Knotsx and knotsy are vectors of the knot locations, and knots of multiplicity k are used at the end of the intervals. The spline order k is 3 for quadratic splines. The grid points for the data to be fit are defined by vectors y and x, and the gridded data is in the matrix Z.
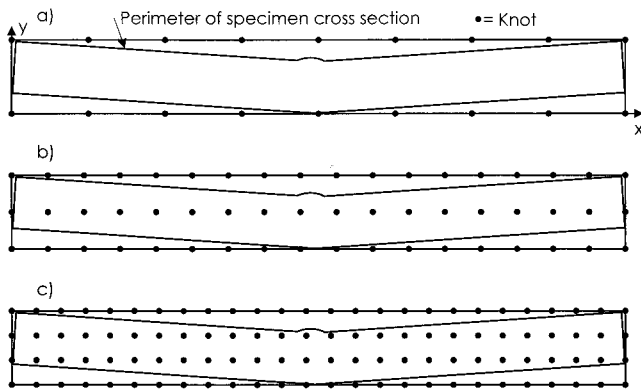
Fig. 4—Refining the surface fit by increasing the number of knots for the smoothing splines. The top (a) shows the coarsest grid, and the middle (b) and bottom (c) show the next two finer grids

Fig. 5—The optimal knot spacing in the bivariate smoothing spline was determined by minimizing uncertainty in the calculated stresses

In this study, the approach to determine the optimum spline smoothing involved incrementally increasing the knot density and calculating the stresses for each increment. First, a single interval, bounded by two knots, was used in the shortest dimension of the cross section, y. The knots in the x-direction were then chosen to have the integral number of intervals giving the spacing closest to that in the y-direction (see Fig. 4(a)). Note that a regular grid of knots was required, so the data were fit over the smallest rectangle that circumscribed the cross-section of the weld plate. Using the fit to the data from this knot grid, stresses on the cut plane were calculated with the FE model. The process was repeated with refined knot spacing by adding another interval in the y-direction and a proportional number in the x-direction (see Fig. 4(b)), and the stress calculation was repeated with the new data fit. The uncertainty, $\partial\sigma$, in the calculated stresses at a given node was estimated by taking the standard deviation of the new stress and the stress from the previous, coarser fit. This standard deviation of two values is given by

$$\partial\sigma\,(i,\,j) = \frac{1}{\sqrt{2}}\,|\sigma\,(i,\,j) - \sigma\,(i,\,j-1)|, \qquad (1)$$

where $\sigma(i,\,j)$ is the stress at node i for the smoothing spline solution designated j, and $j-1$ refers to the previous, coarser smoothing-spline solution. Finally a global or average uncertainty over the whole stress map is given by the root-mean-square (rms) of all the nodal uncertainties

$$\overline{\partial\sigma}\,(j) = \frac{1}{\sqrt{n}}\sum_{i=1}^{n}\partial\sigma\,(i,\,j), \qquad (2)$$

where n is the number of FE nodes on the cut surface in the model. The process of increasing the number of knots, fitting the data, calculating the stresses, and estimating the average uncertainty, $\overline{\partial\sigma}$, was repeated (e.g., Fig. 4(c)) until there was almost one knot per millimeter.

Figure 5 shows how a density of about 0.4 knots mm^{-1} was chosen as giving the optimum amount of smoothing. The curves with the filled symbols show that increasing the knot density always results in better fits to the data, evaluated by taking the rms difference between the smoothed and actual data. The curves with the open symbols show, however, that
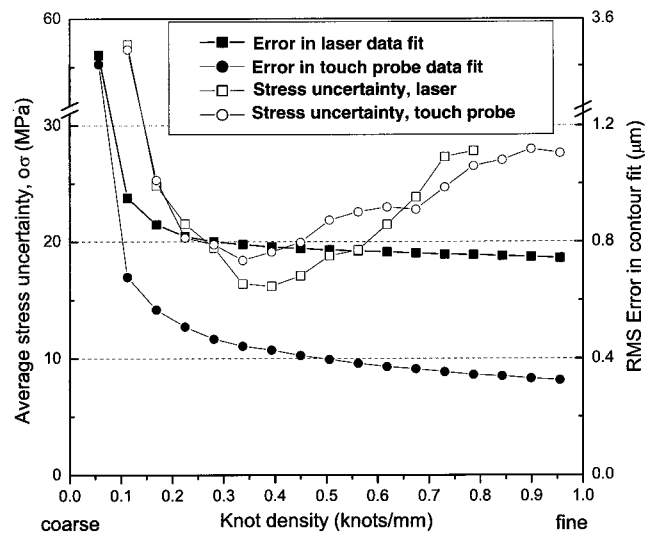
the uncertainty in the calculated stresses as given by eq (2) has a minimum. This minimum occurs at a knot density soon after the curvature in the solid-symbol curves becomes quite small. This region can easily be qualitatively identified as the elbow in curve, and a similar region has previously been found to be the region of optimal data fit when calculating stress.[23] For the contour measured using the laser, the minimum stress uncertainty of 16 MPa occurs at 0.4 knots mm^{-1}. For the contour measured with the touch probe CMM, the minimum of 18.4 MPa occurs at 0.34 knots mm^{-1}. To keep the comparison as straightforward as possible, results for the touch probe CMM measurement will be reported at 0.4 knots mm^{-1}, the same as the laser, where the uncertainty increases negligibly to 19 MPa. The fact that the optimal knot spacing for the touch probe data is approximately the same as for the laser data in spite of the significant difference in the number of raw data points indicates that the optimal amount of smoothing is, within bounds, a function of the physical features of the stress variation and the resulting contour rather than a function of the number of data points. At 0.4 knots mm^{-1}, a spline spans 2.5 mm, which indicates that features in the surface contour are being captured to a resolution of about 1–2 mm.

Further confidence in the selection of the optimal smoothing can be provided by examining the behavior of interior extrema in the calculated stress map. Figure 6 shows how the peak tensile residual stress in the calculated stress maps varies with knot density. At suboptimal knot densities, the maximum stress has not converged to its final value. At supraoptimal knot densities, the peak stress becomes unstable and grows as the peak localizes to an increasingly smaller area. However, over a fairly wide range of knot densities, in precisely the region selected as optimal, the peak stress is relatively stable. In the stable range identified in Fig. 6, the peak stresses are about 730±20 MPa and 750±20 MPa for the laser and touch probe results, respectively. An equivalent examination of the peak compressive stresses does not give similar insight because of the location of the peak. The peak tensile
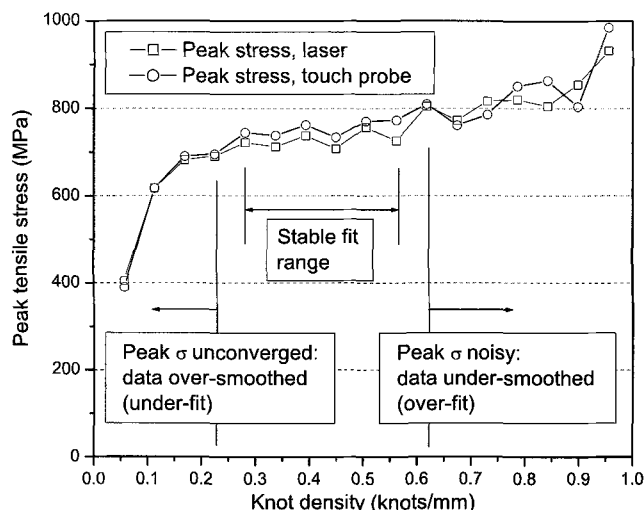
Fig. 6—The peak tensile stress in the calculated stress map is relatively stable for a range of knot densities bracketing the optimum knot density

stress is in the interior of the part's cross-section, as is shown below in the Results section. The peak compressive stress, however, occurs on the perimeter. The data extrapolation and smoothing process make these calculated perimeter stresses less stable.

Results

Figure 7 shows the cross-sectional maps of residual longitudinal stresses measured by both the contour and neutron diffraction methods. The agreement between the two contour method maps is excellent, indicating that the result on this specimen is independent of the experimental method used to measure the surface contour. The agreement between the contour method and neutron diffraction stress maps is also very good. The differences are within the bounds expected based on the uncertainty estimates, providing a convincing cross validation of both the contour and neutron diffraction techniques. Further confidence in the comparison is given by observing that the differences between the contour method and neutron diffraction results fall within the experimental scatter when this weld specimen was measured at six different neutron laboratories (see Fig. 3 in reference 15). The uncertainties given in Fig. 7 are greater than the values from Fig. 5 because of additional sources of uncertainty, the calculations of which are beyond the scope of this paper. These final uncertainties are lower with the laser than the touch probe because the greater number of data points made the results less sensitive to random noise in the data.

Several interesting features are apparent in the stress maps and are consistent between the contour and neutron measurements. To help interpret the results, Fig. 7 shows the outline of the weld region and heat-affected zone (HAZ) as determined through metallographic analysis. The peak tensile stresses of about 740 MPa occur at roughly the center of the weld, and they exceed the reported, as-welded yield strength of 525 MPa for the filler metal. The peak stresses occur subsurface and exceed the yield strength for largely the same reason; the stress is highly triaxial in this region. Individual

residual stress components exceeding yield strength because of triaxiality have been observed routinely in tensile stress regions of welds.[24] The tensile stresses in the surface region of the weld are greater on the +x side of the weld as a consequence of the order of the welding passes and the removal of the constraints for the last two passes (the last pass produced the protruding bead). A second tensile stress peak is observed near the bottom surface, opposite the weld. Additionally, the far-field tensile stress region at the +x end of the cross-section is wider than the region at the −x end as a result of variations in the flame-cutting process that was used to cut the plate from a larger piece of material.

Discussion

Laser Contouring

There are several advantages to using laser probe scanning over a touch probe even though this study reports excellent agreement between the two. In order to validate the laser system, a test specimen was chosen where the touch probe would perform well. The specimen was fairly large and had high residual stresses, resulting in a large contour that could easily be measured using a touch probe. In cases where the magnitude of the surface contour is smaller, the touch probe would be outperformed by the laser system because of increased resolution in height detection. This extends the useful range of the contour method to smaller parts with more subtle stresses. In work to be reported in the future, the laser system has already enabled the measurement of moderate stresses in a dissimilar aluminum-alloy friction stir weld where a touch probe was unsuccessful. Another advantage of laser contouring is its high rate of data acquisition. The fast data collection enables one the luxury to increase point density and perform real time point averaging. Higher point density better defines the surface contour, and point averaging improves the probe's precision by compensating for vibrations and other stochastic noise errors that can be difficult to control otherwise. Furthermore, a commercial laser contouring system currently costs roughly half as much as the best touch probe CMMs because the CMM includes the added capability of full three-dimensional measurement.

The non-contact nature of a laser system can also be an important advantage over a touch probe. The touch probe measurements reported in this work used the default contact force, which is nominally quite light, and the measured material, steel, is relatively hard. Even so, the surface was damaged. A visual inspection of the surface after measurement showed that the location of each touch probe measurement point was visible because of deformation at the contact point. For softer materials, more damage could be expected.

A triangulation probe can also be used for the surface contouring, although the confocal probe used in this work was preferred largely because it is insensitive to optical surface variations prevalent on EDM surfaces. A triangulation probe measures displacement by forming a focused laser spot on the target surface, imaging the spot by lenses onto a solid-state detector, and determining height by triangulation.[25] Unfortunately, a triangulation probe can have difficulty measuring a dark surface, which often occurs with EDM. An active confocal probe measures displacement by actively finding the laser focus at the target surface.[26] Relative to the best confocal probes, the best triangulation probes have the advantage of higher resolution and data acquisition speed. The
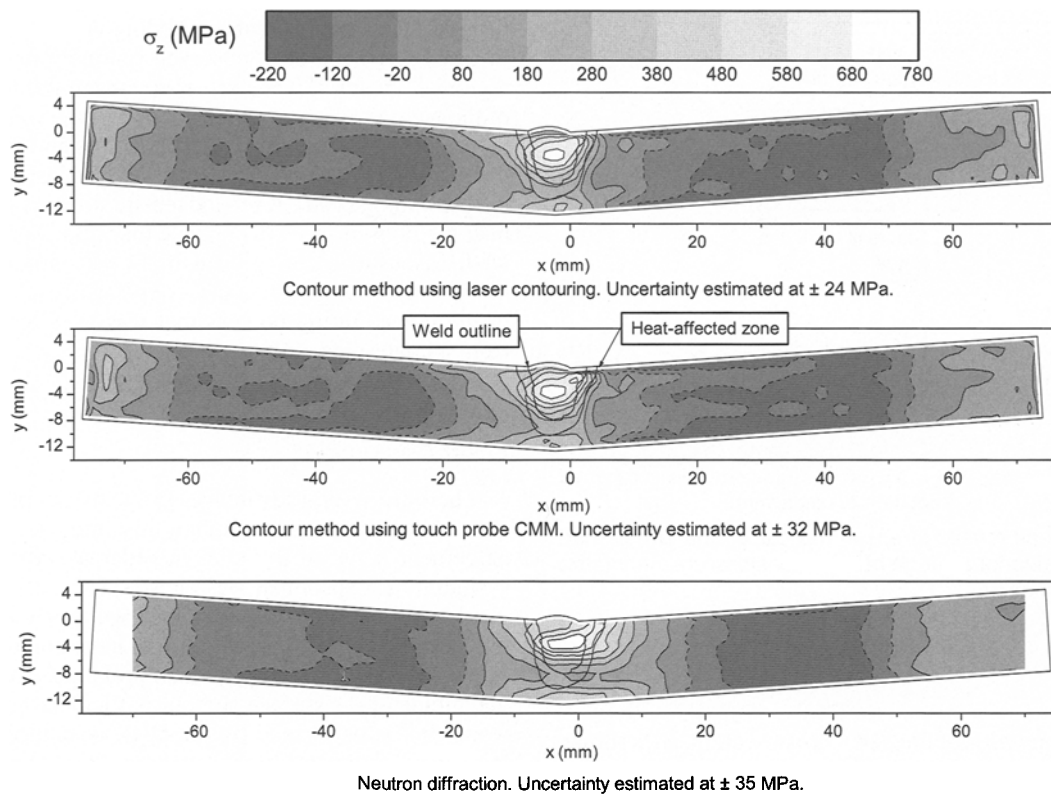
Fig. 7—The stress maps measured with the contour method and neutron diffraction. Dashed lines are used for compressive stress contours and solid lines for tensile

confocal probe's 0.4 μm resolution (at 4000 points s^{-1} sampling rate) is adequate for this work, even though we have often achieved usable results using triangulation probes on the same surfaces.

The Contour Method in General

The results in this paper indicate that the contour method may be less sensitive to yielding than other relaxation methods. The contour method, like most relaxation methods, assumes that the stress relaxation process is elastic. However, high-magnitude residual stresses could possibly lead to yielding as the stresses are released during cutting. The measured peak residual stresses in the weld plate, $\sigma_z = 740$ MPa, exceed the filler material's nominal yield strength of about 525 MPa. Yet the contour method results agree very well with the results of neutron diffraction, in which there is no relaxation for yielding to occur. Thus, the agreement between the two measurements indicates that yielding did not affect the contour method results. Qualitatively, yielding is minimal in the contour method measurement because relaxation involves *unloading* of stresses, which is usually elastic, and because strain hardening has likely increased the local yield strength in stressed regions to above the nominal 525 MPa. Recent experimental studies with the hole-drilling method have confirmed that yielding does not necessarily occur in relaxation measurements even when the residual stresses exceed the nominal yield strength of a material.[27] Maybe more importantly, the peak measured σ_z is a poor measure of the amount that the stresses have relaxed. The same FE calculation that gives the map of the stress component normal to

the cut, σ_z, also correctly reveals how the other stress components have changed during unloading.[1] For the stress map in Fig. 7, the Von Mises effective stress only unloaded by 560 MPa, which is a better value to compare with the yield strength. In contrast, the hole-drilling method would tend to be more sensitive to yielding because the stress concentration caused by the hole magnifies the relieved stresses such that the relaxed effective stress is greater.

The results on the weld plate also confirm that the contour method can be applied without a correction for curvature in the WEDM cut surface. In a previous test, an unfortunate choice of material for the EDM wire resulted in the cut surface being slightly curved even for a cut in stress free material.[1] On the weld plate in this paper, a measurement of a test cut in a stress-free region of the plate indicated that the surface was flat to within about 1 μm.

Spline Smoothing and Uncertainty Estimation

The curves with closed symbols in Fig. 5 might give the erroneous impression that the touch probe data are better than the laser data because they are fit better by the same smoothing spline fit. Figure 8 shows comparable traces, or portions of the measured contour, for the laser and touch probe data. Rather than being noisy data, the laser is apparently doing a better job of measuring actual surface roughness. The higher number of data points of the laser data makes it clear that there are trends in the data rather than random noise. Careful examination of the touch probe data, keeping in mind that the locations of the two traces do not coincide perfectly, indicates that the touch probe data show many features corresponding
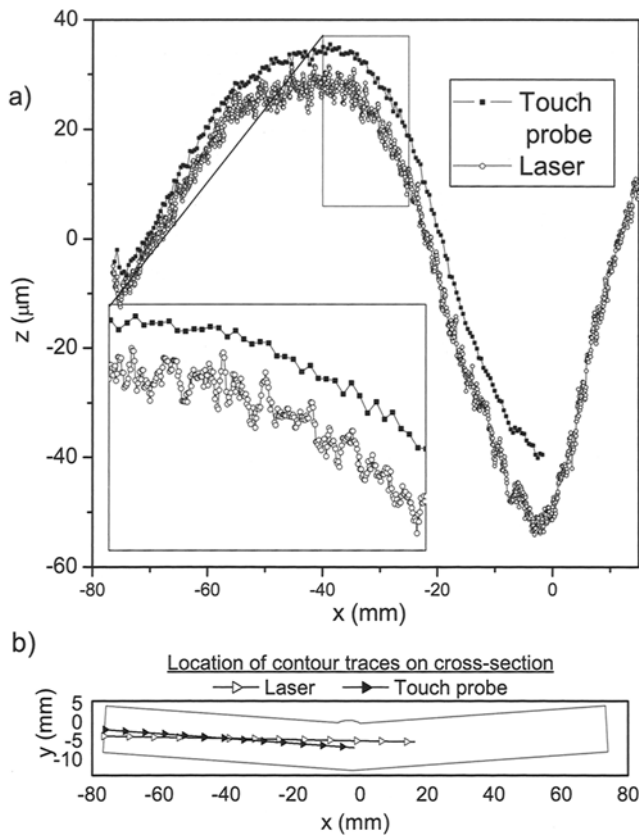
Fig. 8—(a) The laser data seem more noisy than the touch probe data because the laser measures surface roughness more precisely. The two plotted contour traces, locations shown in (b), are offset in the z-direction to make the plot clearer

to the trends in the laser data. The lower spatial resolution (in the x-direction in Fig. 8) of the touch probe data makes it difficult to distinguish these features from random noise. Also, the finite radius of the probe tip effectively decreases the magnitudes of the peaks, smoothing the data and reducing the rms error in the smoothing fit. Similar smoothing of local surface roughness peaks could be accomplished with the laser by adjusting the data sampling and averaging rates. However, both data sets require further smoothing anyway.

Equations (1) and (2) only give an estimate of one part of the total uncertainty in the measured stresses, but that one part was appropriately used to choose the optimal amount of smoothing of the measured contour data. These equations estimate the uncertainty caused by fitting the measured surface contour data to a particular functional form, in this case bivariate splines. Such uncertainty is often referred to as "model error". Hence, the optimal amount of spline smoothing, i.e., the optimal model, was chosen by minimizing this error.

It is likely possible to simplify the determination of optimal smoothing. The calculational burden could be minimized by calculating the fit error as a function of smoothing (the solid symbols in Fig. 5; a quick calculation), and then restricting the more costly stress calculations to the region of the elbow in the curve. Furthermore, other smoothing splines that might be more convenient could be used, such as ones that smooth based on a smoothing parameter instead of knot den-

sity. However, determining optimal knot density gives useful estimates of the spatial scale of the stress variations and of the required mesh density for the FE calculations.

Conclusions

The ability of the contour method to measure a cross-sectional residual stress map with intricate spatial variations has been verified by comparing contour method results with neutron diffraction results in a weld plate. The contour method is a significant addition to the range of techniques currently used to measure residual stress, all of which have their particular advantages and limitations. The biggest advantages of the contour method, compared to the few other methods that can measure a comparable stress map, are that it is relatively simple and inexpensive to perform and the equipment required is widely available.

Non-contact laser surface contouring improves the capability of the contour method by allowing higher resolution measurement of a surface contour. The increased resolution occurs both in the accuracy of the measured surface height and in the density of data points that can be taken conveniently. This increased resolution will allow the contour method to measure residual stresses more accurately and/or measure smaller parts or parts with lower stress levels than was previously possible. Conventional touch probe technology, usually on a CMM, can still be used for cases where the extra resolution is not required.

Spline smoothing proved to be a versatile and effective method to fit and smooth the data and to estimate uncertainties. This approach has been very useful for measuring spatially intricate stress maps.[28] Most importantly, this approach provided an objective method to smooth the data and calculate the stresses unambiguously. When such rigor is not of paramount concern, simpler methods can be used.

Because the deviations from the assumption of a flat cut are greater than the uncertainty in the laser measured contour, making the cut now limits the accuracy and resolution of the contour method. With WEDM, one of these deviations is roughness of the cut surface. Other deviations occur because of the finite (non-zero) width of the cut. With current WEDM technology, these errors can be minimized by using the gentlest cut settings and by using a smaller wire. In the future, improvements in WEDM technology or the use of other advanced machining processes to make the cut could improve the sensitivity and resolution of the contour method even further.

References

1. Prime, M.B., "Cross-sectional Mapping of Residual Stresses by Measuring the Surface Contour After a Cut," Journal of Engineering Materials and Technology, 123 (2), 162–168 (2001).
2. Prime, M.B., U.S. Patent 6,470,756 (2002).
3. Withers, P.J. and Bhadeshia, H.K.D.H., "Overview—Residual Stress Part 1—Measurement Techniques," Materials Science and Technology, 17 (4), 355–365 (2001).

4. Smith, D.J., Bouchard, P.J., and George, D., "Measurement and Prediction of Residual Stresses in Thick-section Steel Welds," Journal of Strain Analysis for Engineering Design, **35** (4), 287–305 (2000).

5. Virkkunen, I., "Thermal Fatigue of Austenitic and Duplex Stainless Steels," Doctoral Dissertation at Helsinki University of Technology (2001).

6. Zhang, Y., Fitzpatrick, M.E., and Edwards, L., "Measurement of the Residual Stresses around a Cold Expanded Hole in an EN8 Steel Plate Using the Contour Method," Materials Science Forum, **404–407**, 527–532 (2002).

7. Prime, M.B. and Martineau, R.L., "Mapping Residual Stresses After Foreign Object Damage Using The Contour Method," Materials Science Forum, **404–407**, 521–526 (2002).

8. Kaplan, H., "Laser Gauging Enters a Submicron World," Photonics Spectra, **31** (6), 67–68 (1997).

9. Zhao, Z.B., Hershberger, J., Yalisove, S.M., and Bilello, J.C., "Determination of Residual Stress in Thin Films: A Comparative Study of X-Ray Topography Versus Laser Curvature Method," Thin Solid Films, **415** (1–2), 21–31 (2002).

10. Nelson, D.V. and McCrickerd, J.T., "Residual Stress Determination Through Combined Use of Holographic-interferometry and Blind-hole Drilling," EXPERIMENTAL MECHANICS, **26** (4), 371–378 (1986).

11. Wang B.S., Chiang, F.P., and Wu, S.Y., "Whole-field Residual Stress Measurement in Rail Using Moire Interferometry and Twyman/Green Interferometry Via Thermal Annealing," EXPERIMENTAL MECHANICS, **39** (1), 71–76 (1999).

12. Pechersky, M.J., Miller, R.F., and Vikram, C.S., "Residual Stress Measurements with Laser Speckle Correlation Interferometry and Local Heat-Treating," Optical Engineering, **34** (10), 2964–2971 (1995).

13. Buitrago, J. and Durelli, A.J., "Interpretation of Shadow-moire Fringes," EXPERIMENTAL MECHANICS, **18** (6), 221–226 (1978).

14. Pirodda, L., "Shadow and Projection Moire Techniques for Absolute or Relative Mapping of Surface Shapes," Optical Engineering, **21** (4), 640–649 (1982).

15. Hughes, D.J., Webster, P.J., and Mills, G., "Ferritic Steel Welds—A Neutron Diffraction Standard," Materials Science Forum, **404–407**, 561–566 (2002).

16. Webster, P.J., "The Neutron Strain Scanner," Kerntechnik, **56**, 178–182 (1990).

17. Benedict, G.F., Nontraditional Manufacturing Processes, Marcel Dekker, New York (1987).

18. Cheng, W., Finnie, I., Gremaud, M., and Prime, M.B., "Measurement of Near Surface Residual Stresses Using Electric Discharge Wire Machining," Journal of Engineering Materials and Technology, **116** (1), 1–7 (1994).

19. Sebring, R., Anderson, W., Bartos, J., Garcia, F., Randolph, B., Salazar, M., and Edwards, J. "Non-contact Optical Three Dimensional Liner Metrology," Proceedings of the 28th IEEE International Conference on Plasma Science and The 13th IEEE International Pulsed Power Conference, Las Vegas, NV, June 17–22, 2001, 1414–1417 (2001).

20. DeWald, A.T. and Hill, M.R., "Residual Stress in a Thick Steel Weld Determined Using the Contour Method," University of California, Davis report for Los Alamos National Laboratory Contract 32390-001-01-49 (October 2001).

21. DeBoor, C., MATLAB Spline Toolbox User's Guide, The Math Works, Inc., Natick, MA (2000).

22. Cao, Y.P., Hu, N., Lu, J., Fukunaga, H., and Yao, Z. H., "An Inverse Approach for Constructing the Residual Stress Field Induced by Welding," Journal of Strain Analysis for Engineering Design, **37** (4), 345–359 (2002).

23. Hill, M.R. and Lin, W.Y., "Residual Stress Measurement in a Ceramic-metallic Graded Material," Journal of Engineering Materials and Technology, **124** (2), 85–191 (2002).

24. Webster, G.A. and Ezeilo, A.N., "Residual Stress Distributions and Their Influence on Fatigue Lifetimes," International Journal of Fatigue, **23** (SS), S375–S383 (2001).

25. Gasvik, K.J., Optical Metrology, 2nd edition, Wiley, Chichester, UK (1995).

26. Dainty, J.C., Current Trends in Optics, Academic, San Diego, CA (1994).

27. Nobre, J.P., Kornmeier, M., Dias, A.M., and Scholtes, B., "Use of the Hole-drilling Method for Measuring Residual Stresses in Highly Stressed Shot-Peened Surfaces," EXPERIMENTAL MECHANICS, **40** (3), 289–297 (2000).

28. Prime, M.B., Newborn, M.A., and Balog, J.A., "Quenching and Cold-Work Residual Stresses in Aluminum Hand Forgings: Contour Method Measurement and FEM Prediction," Materials Science Forum, **426–432**, 435–440 (2003).